Received: 3 February 2023 | Revised: 17 April 2023 | Accepted: 19 April 2023

DOI: 10.1002/eng2.12667

RESEARCH ARTICLE

Engineering Reports Open Access WILEY

Iron deficiency anemia detection using machine learning models: A comparative study of fingernails, palm and conjunctiva of the eye images

Justice Williams Asare[1] | **Peter Appiahene**[1] | **Emmanuel Timmy Donkoh**[2] | **Giovanni Dimauro**[3]

[1]Department of Computer Science and Informatics, University of Energy and Natural Resources, Sunyani, Ghana

[2]Department of Basic and Applied Biology, University of Energy and Natural Resources, Sunyani, Ghana

[3]Coordinatore del Consiglio di Interclasse dei Corsi di Studio in Informatica. Dipartimento di Informatica, Università degli Studi di Bari 'Aldo Moro', Bari, Italy

Correspondence
Justice Williams Asare and Peter Appiahene, Department of Computer Science and Informatics, University of Energy and Natural Resources, Sunyani, Ghana.
Email: justice.asare.stu@uenr.edu.gh and peter.appiahene@uenr.edu.gh

Abstract

Anemia is one of the global public health challenges that particularly affect children and pregnant women. A study by WHO indicates that 42% of children below the age of 6 and 40% of pregnant women worldwide are anemic. This affects the world's total population by 33%, due to the cause of iron deficiency. The non-invasive technique, such as the use of machine learning algorithms is one of the methods used in the diagnosis or detection of clinical diseases, which anemia detection cannot be overlooked in recent days. In this study, a machine learning approach was used to detect iron-deficiency anemia with the application of Naïve Bayes, CNN, SVM, k-NN, and decision tree algorithms. This enabled us to compare the conjunctiva of the eyes, the palpable palm, and the color of the fingernail images to justify which of them has a higher accuracy for detecting anemia in children. The method utilized was categorized into three different stages: dataset collection, dataset preprocessing, and model development for anemia detection. The CNN achieved a higher accuracy of 99.12%, while the SVM had the least accuracy of 95.4%. The performance of the models justifies that the non-invasive approach is an effective mechanism for anemia detection.

KEYWORDS

anemia, data augmentation, iron deficiency, non-invasive, region of interest

1 | INTRODUCTION

Anemia is a serious public health problem that mostly affects children and pregnant females globally. A study by the WHO indicates that 42% of children below the age of 6 and 40% of females who are pregnant worldwide are anemic.[1,2] Anemia affects the world's population of 33% due to iron deficiency.[3] Anemia occurs once the level of red blood cells within the body decreases or when the structure of the red blood cells is destroyed or weakened.[4]

It is also possible to confirm the diagnosis or to detect anemia by measuring the amount of hemoglobin in the blood or the hematocrit, which quantifies the ratio of red blood cells to total blood volume. Those whose hemoglobin or hematocrit levels are more than two standard deviations below the normal range are deemed to have anemia.[5]

Throughout the pregnancy period, the plasma level is reduced to 50%, while the mass ranges from 18% to 20% in Hb and red blood cells to 33%.[6] A procedure that is complex and comprehensive takes place in the human body for the regeneration of red blood cells after the loss of blood. Anemia can also occur when the Hb level in the red blood cell is below the normal threshold, which results from one or more increased red cell destruction, blood loss, defective cell production or a depleted sum of red blood cells.[7] Early detection symptoms of anemia are an ideal primary stage to alleviate it because if the detection and treatment of anemia are delayed, it irreversibly damages the human organ, which can lead to death in some instances.[8]

Hb carries oxygen from the lungs to tissues, and carbon dioxide is returned from the tissue of the lungs, which is considered to be an essential task in the human body. This also performs an estimation of the Hb level for analysis of blood to detect either one is anemic or not. The level of Hb usually determines whether one is anemic or not.[9]

Iron deficiency anemia has additionally been shown to affect psychological features and physical development in children and cut back productivity in adults.[10,11] Long-term illness can also contribute to a patient's risk of diagnosing anemia. Syndromes that mingled with the sophisticated prevalence of anemia include diabetes, kidney syndrome, cancer, human immunodeficiency virus, inflammatory bowel disease, and cardiovascular disease.[12] Malaria, bilharzia, and hemoglobinopathies are other main contributors.[1,12]

The clinical approaches used for the detection of anemia are based on the extraction of blood, which requires higher labor and costs of instrumentation and is a time-ingesting technique that exposes health workers to blood-transmissible diseases.[13] In numerous health centers, evaluation of the conjunctiva pallor is usually used to detect anemia that turns out to be rapid. Medical officers usually pull down the protective fold (the lid of the eye) and subjectively assess or examine the color of the conjunctiva of the eye.[9,14]

In several cases, the clinical sign for the detection of anemia will be quite helpful, but the lack of agreement between observers on several things and the low sensitivity of the conjunctiva color will undermine the authenticity of the visual detection method.[15,16] This examination is not precise and is not reliable since the quality of these findings depends on the decision and training of the health officer.[17]

Numerous emerging geographical areas are vulnerable to anemia due to inadequate health and medical facilities with few health workers, such as medical officers and laboratory technicians or biomedical scientists. The potential risk of anemia can be diagnosed and monitored by using the non-invasive method and smartphone-based devices which is cost-effective, takes less time, and is more promising in focusing on these health issues.[17] This state of affairs may be lessened without the involvement of blood assessment that is costive and inaccessible in several areas which makes the detection of anemia complex in its early stage.[13]

This study aims to detect anemia using a non-invasive method, which is a comparative study of machine learning algorithms (Naïve Bayes, CNN, SVM, k-NN, and decision tree) with the use of images of the palpable palm, the color of the fingernails and conjunctiva of the eyes. Since timely detection and treatment of anemia improves population health outcomes, physical capacity building, and well-being, resulting in increased economic growth.[18]

The major contribution to this study is the use and combination of three (3) different dataset, that is, the conjunctiva of the eye, palpable palm and color of the fingernail images for the detection of iron deficiency anemia. In addition, this study compared the performance of five (5) machine learning models while most studies applied a single model or two to detect anemia. Lastly, the size of our dataset used for this study. We used the largest publicly available dataset of 710 images for each class to assist in the development of machine learning models for the detection of iron deficiency anemia. Our dataset has a balanced class of both anemic and non-anemic images from 10 different hospitals in Ghana as indicated in Appendix Table A1.

2 | RELATED WORKS

In recent times, the use of computerized algorithms such as machine learning for the estimation of Hb and the diagnosing or detection of medical diseases such as anemia is commonly related with high accuracy to analyzing the color of nailbeds, conjunctiva of the eyes and the palpable palm from digital photographs taken by smartphones.[19] By classifying the basic set of algorithms, the quintessence of the classification method types such as the support vector machine (SVM), K-nearest neighbor (k-NN), Bayesian networks, artificial neural networks (ANN), and decision tree classifier is considered, showing comprehensive data mining algorithms and a group of their essentiality type.

For detecting anemia using a non-invasive method, a lot of research has been conducted using conjunctiva images of the eye.[20] indicated that specifically the best algorithms for classification or detection are based on the domain of the problem to be solved. However, there are limited attributes used for only a few blood parameters.[21]

The study conducted by Peksi et al.[22] used a non-invasive technique to detect anemia with the help of clinical symptoms based on fingernails and palm images with their intensity color. They extracted the RGB component of 20 images and utilized the Naïve Bayes algorithm which achieved an accuracy of 90%. Verma and Arjun[23] used different attributes that included age, sex, symptoms, chronic diseases, and blood parameters in consultation with experienced medical consultants. The study utilized notable methods such as ANN, SVM, and decision tree-based methods and Naïve Bayes, K-NN and rule-based approaches was applied to the Hb value.

A SVM approach was utilized[8,24] to computerize a non-invasive model to detect anemia using 19 conjunctivae of the eye images. The images corresponded to their various hemoglobin levels known, which attained an accuracy of 78.90% in 15 out of the 19 cases. Irum et al.[24] used the least squares support vector machine (LS-SVM) to detect anemia using conjunctiva images of the eyes using the application of image processing and computer vision. The procedure resulted in a precision of 85%, a sensitivity of 92%, and a specificity of 70%. The study used 77 tested images, of which 21 were non-anemic while 56 were anemic.

With the use of conjunctiva of the eye images, Chen et al.[25] proposed a machine learning technique for anemia detection. The system achieved a confidence interval of 95 after it was trained and tested on the conjunctiva of the eye images. Based on the correlation between anemia symptoms and patients' emotional posts on the Twitter platform, Sarsam et al.[26] established a novel method for detecting anemia. The study's prediction accuracy was 98.96% through the use of the k-means and latent Dirichlet allocation algorithms.

Shahzad et al.[27] developed a three-tier deep convolutional fused network (3-TierDCFNet) to extract optimal morphological characteristics from anemic photos to predict anemia severity. The proposed model was divided into two modules: Module-I assessed the input picture as anemic or non-anemic, whereas Module-II recognized the anemia severity level and classified it as mild or chronic. The study by Karagül et al.[21] used hemoglobin, and hematocrit with corresponding patients' biodata acquired from the Düzce University Hospital in Turkey. The study aimed to develop a system that will detect anemia under conventional clinical practice conditions that required multi-class analytical results using machine learning algorithms.

A study conducted by Yeruva et al.[28] aimed to compare anemic and non-anemic images for the detection of anemia with the application of k-NN, SVM and decision tree algorithms. The study utilized images of the conjunctiva of the eyes, and blood samples were used to measure the Hb values of patients as an auxiliary dataset to the images. For enhancement of the dataset, the images were preprocessed, transformed with noise filters, and converted to gray images. The decision tree algorithm achieved an accuracy of 95% which was higher than the SVM and the k-NN performance of 80% and 83% respectively.

Dimauro et al.[29] in their study proposed a novel pipeline for anemia detection that aimed to verify the hypothesis that the paleness of the sclera and blood vessels in the sclera may be considered symptoms of anemia. The study used conjunctiva of the eye images of 218 participants aged 19–88 years. The study concluded that the color of the sclera and scleral blood vessels can be used to detect anemia with an accuracy of 86.4%. In the study conducted by Dada et al.[30] a CNN model was used to develop cost-effective and controllable applications for the detection of anemia which achieved an accuracy of 89.33%. In the application of convolutional neural network (CNN) batch normalization layers normalize the activation and gradients propagating across the network, allowing network training to be optimized, while ReLU layers develop network training and decrease network affectability.[30,31]

Ghosh et al.[32] estimated the quantity of Hb level with the application of ANN and the use of biodata, extracted blood samples and images from 86 patients. The feature description of the samples was used to calculate the color intensity from the extracted blood images. The study achieved a sensitivity of 95.50% and a specificity of 52% when the features were obtained from the collected dataset which was used to feed the proposed ANN model. According to a study by Dimauro et al.[29] the diagnosis of anemia using a non-invasive approach is a cost-effective and reliable method and is now an important research issue since it avoids patients from experiencing pain from physical examinations and clinical laboratory testing. The "Eyes-defy-anemia dataset," which includes 218 images of the conjunctiva of the eye from Italy and India was utilized in the study. Palpebral conjunctiva pictures were used to train the system, and the results showed 88% accuracy, 0.66 sensitivity, 0.91 specificity for the Italian dataset, and 75% accuracy, 0.79 sensitivity, and 0.74 specificity for the Indian dataset.

Similarly, Rojas et al.[33] compared the results of their study with those of the laboratory test that yielded a sensitivity and specificity of 91.89% and 85.18%, respectively, when images of the conjunctiva and tongue were used with the

application of logistic regression and neural network algorithms, while, Delgado-Rivera et al.[34] applied the neural network of convolution with the aid of segmented images of the conjunctiva to detect amenia, which obtained a sensitivity of 77.58%. The results were compared with laboratory tests. Furthermore, Dimauro et al.[10] detected anemia using the image of the conjunctiva of the eyes. A new device for image capture was proposed based on the use of the k-NN algorithm, which achieved 90.26% accuracy using nonanemic images of 84 patients and anemic images of 29 patients. Appiahene et al.[7] stated that the use of the conjunctiva alone to detect anemia in children is not enough, as exposing the conjunctiva could expose them to germs, bacteria, or falling objects; hence, the use of the palpable palm was recommended.

An automated system for detecting cataract disease with the use of color of the fundus images was proposed by Acar et al.[35] A deep learning-based approach, that is, VGGNet and DenseNet architectures was utilized for the study to also detect anomalies for the description of the region of interest (ROI) in the human eyes when extracting the ROI of the conjunctiva of the images. The proposed system archived an accuracy of 97.94% and 95.07% by the VGGNet by DenseNet respectively in the diagnosis of cataract disease. Table 1 gives a summary of some related works showing the dataset, technique or method used and their contribution or accuracy obtained in the study.

Gaps in the related works above include the size of the dataset used for the studies. Most studies such as References 8,22,38 used a small-size of dataset without the use of image augmentation which could affect the performance of the study. This is because machine learning models perform better when trained, validated and tested on huge dataset samples.[7,37] In addition, most of the studies in the related work applied a single model and as a result, the performance of the model was not compared with other models and also uses a single feature such as the conjunctiva of the eye images, except Roychowdhury et al.[38] that used both conjunctiva of the eye and palpable tongue images.

However, this study is based on the application of five (5) machine learning models with the use of 710 conjunctiva of the eye, palpable palm, and color of the fingernail images which were also augmented for effective performance in

TABLE 1 Summary of some related works showing dataset and techniques used, and contributions.

Reference	Dataset used	Preprocessing technique(s)	Feature extraction method used	Algorithm used	Contribution
Tamir et al.[8]	19 conjunctiva of the eye images	Image segmentation	Not indicated	RGB thresholding algorithm	The RGB thresholding algorithms used attained an accuracy of 78.90%
Peksi et al.[22]	Digital images of nails and palms (20 datasets)	Image segmentation	Segmentation was used to calculate the average RGB value of images	Naïve Bayes	The Naïve Bayes obtained 90% accuracy
Yadav and Singh[36]	400 retinal images	PCA-based color conversion, contrast-limited adaptive histogram equalization (CLAHE).	Gray-level co-occurrence matrix (GLCM), Laws' texture energy (LTE)-based, Tamura's features, wavelet features, and HOG features	SVM, k-NN, and decision tree	An accuracy of 77.30% was given by the SVM
Jain et al.[37]	99 images of the conjunctiva	Image augmentation and image segmentation	Manual extraction of ROI of the palpable conjunctiva of the eyes	Artificial neural networks (ANN)	An accuracy of 97.00% was attained by the ANN
Roychowdhury et al.[38]	27 conjunctiva of the eyes and 56 palpable tongue images	Image segmentation	Color Planes and Gradient Feature Extraction (from RGB to HSV transformation, from RGB to Lab transformation, from RGB to YCbCr transformation)	SVM, logistic regression, decision tree, decision, ANN, Poisson regression and k-NN.	86% accuracy for eyes conjunctiva and 98.2% accuracy for palpable tongue with the decision tree algorithms

the detection of anemia. This study in addition compared the performance of the various features of the human body to determine which of them is efficient and effective in detecting iron deficiency anemia in children (aged 6–59 months).

From the reviewed related works, it is evident that non-invasive techniques such as machine learning algorithms are efficient, cost-effective and provide timely results in medical diseases diagnosing such as anemia detection.

Furthermore, since most studies used the conjunctiva of the eyes, this study compared the performance of the conjunctiva of the eyes, palpable palm and color of the fingernails in the detection of anemia. This is because exposure of the conjunctiva of children may be exposed to infections or falling objects and the palm is also one of the important points of the human body for the detection of anemia,[7,39] hence the need to compare its performance (conjunctiva of the eyes, palpable palm, and color of the fingernails) in the detection of anemia.

3 | METHODOLOGY AND EXPERIMENTAL DESIGN

This section deals with the procedure and algorithms used for the proposed models. The method proposed for this study was made up of three stages. Figure 1 illustrates the conceptual framework used for the study, and Figure 2 also presents a flowchart showing the flow of work in the proposed models.

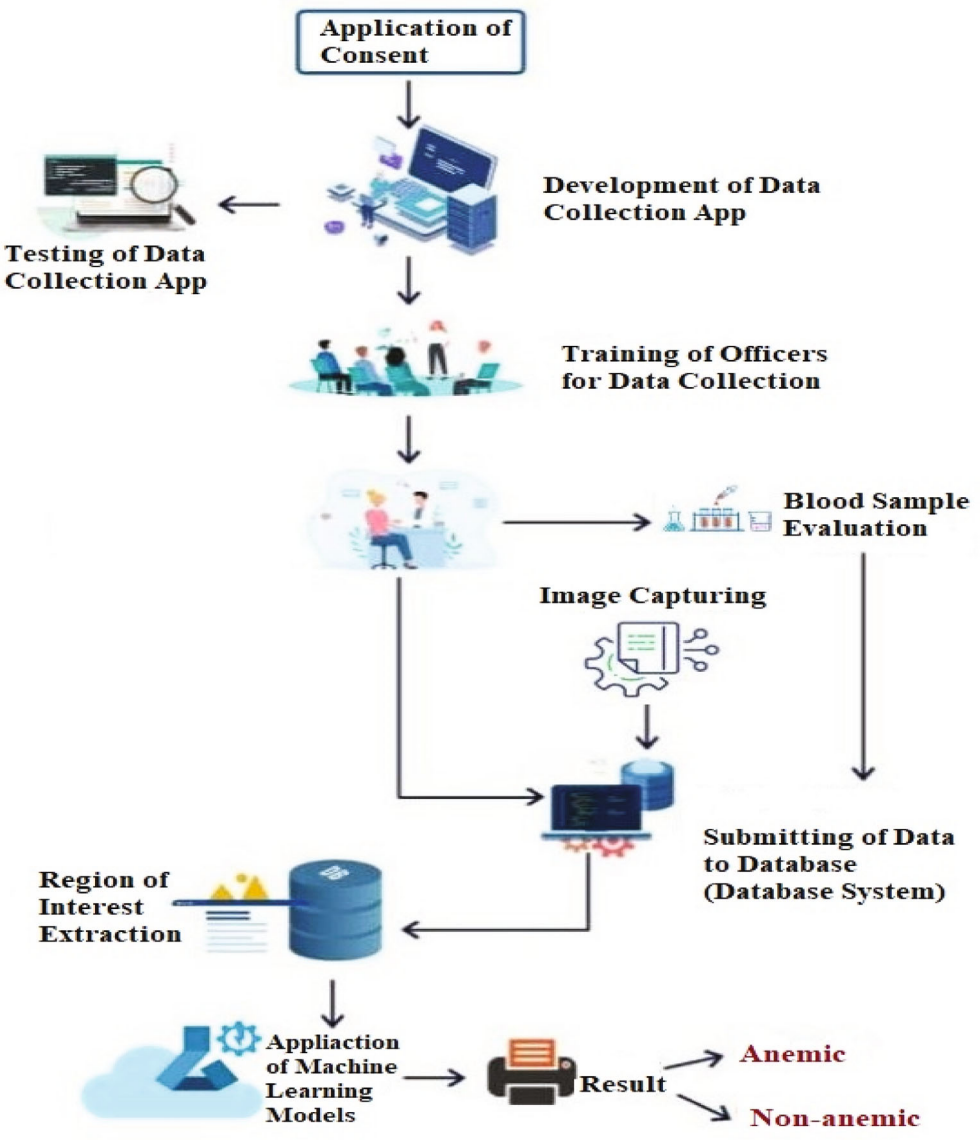

FIGURE 1 A conceptual framework for the proposed methodology.

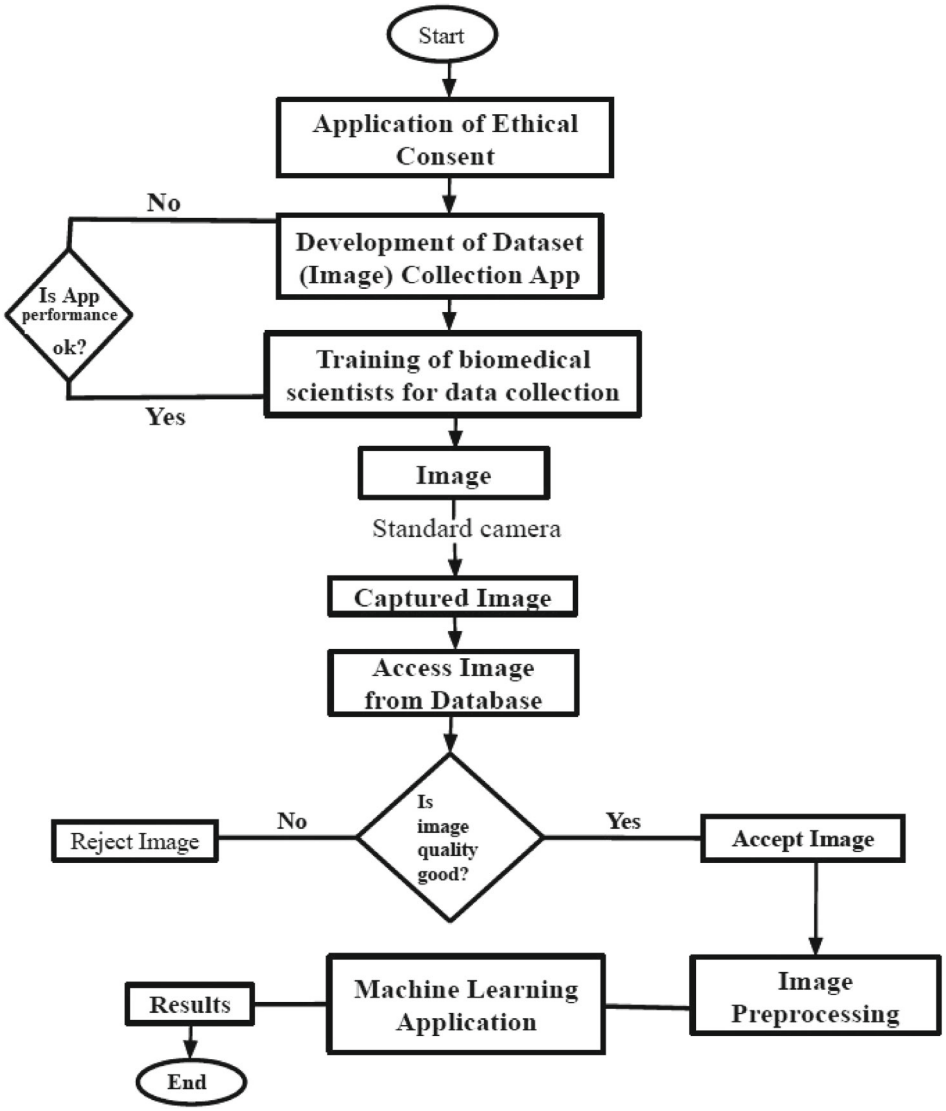

FIGURE 2 A flowchart showing the flow of work in the proposed models.

Stage I: Image capturing (dataset collection); taking images of the palpable palms, conjunctivae of the eyes, and fingernails.

Stage II: Preprocessing of images; extraction of the ROI of the captured images. Afterwards, we separated the component of the CIE L*a*b* (also known as CIELAB) color space of the images, segmented the images, and calculated the mean intensity of the various CIE L*a*b* color space components of the images (extraction and segmentation of the ROI).

Stage III: Development of the detective (anemic or non-anemic) models. Machine learning algorithms (Naïve Bayes, CNN, SVM, k-NN, and decision tree algorithms) were developed to detect anemia using various captured and processed images (datasets).

This means that for anemia to be detected, the dataset goes through three phases or steps.

3.1 | Data collection system and datasets

The system used for data collection was developed using Kobo Collect (v2021.2.4) installed on mobile tablets (Samsung Galaxy Tab 7A). The biodata of the patients/participants such as Hb values, age, sex, and remark (anemic or non-anemic) based on the Hb value captured with the corresponding images (conjunctiva of the eyes, palpable palm and fingernails) and uploaded to the cloud storage (database).

This was carried out by professional (licensed) biomedical scientists who underwent a week-long proficiency training at the Centre for Research in Applied Biology, University of Energy and Natural Resources, Sunyani, Ghana, on how to capture images of children aged 6 to 59 months. The Committee for Human Research and Ethics reviewed and approved (Reference number: CHRE/CA/042/22) this study before its commencement.

Regarding the conjunctiva of the eyes, the lower eyelid was pulled slightly with the thumb and index finger to take the image. On the palm, due to the reason that the participants were children, the biomedical scientists held the hand of the participant and stretched the palm through the fingers and then captured images of the palm. On the fingernails, the wrist hand of the participant was held by the biomedical scientists and a photograph of the fingernails was captured.

However, to avoid disproportionate gleam effects on the image quality that might affect the models' performance, the flashlights of the cameras were off when taking the photographs of the images. This mechanism served as a great measure to eradicate the influence of ambient light in the images.

After the images (datasets) were received through the cloud storage (database), they were extracted using the triangle thresholding algorithm and the images were augmented to increase the data size. Segmentation techniques for ROI extraction comprise dividing an image into multiple segments (i.e., regions) based on distinct characteristics. The thresholding algorithm was a procedure used to divide the image into segments based on a predetermined threshold. The pixels in each image were assigned to one of the three (CIE **L*a*b*** color spaces) segments according to their intensity levels.

With the application of the thresholding algorithm, each image was divided into three classes. Each pixel of the image was then analyzed and the threshold value was applied to determine the color it should be categorized. This process was utilized to extract or isolate the ROI (conjunctiva) from the eye image.

Afterwards, the images were segmented into their various CIE L*a*b* color spaces. The datasets were collected from 10 health facilities across the country (Table A1: List of hospitals). These included districts ($n = 7$), regional ($n = 2$), and tertiary ($n = 1$) hospitals.

This study's dataset focuses on children aged 5–59 months. The datasets used Hb value; <11 g/dL is anemic, while, >=11 g/dL is non-anemic. Figure 3 below shows a sample of how a photograph of the images was taken, where A, B and represents the conjunctiva of the eye, the color of the fingernails and palpable palm images respectively, while Figure 4 shows a sample of the raw (unextracted) dataset used for the study.

In addition, Tables 2 and 3 also show samples of biodata (dataset) collected from selected participants for the study and statistics and characteristics on the original dataset and the Hemoglobin concentration level (g/dL) respectively. Table 2 shows samples of the biodata (dataset) collected from selected participants for the study, while Table 3 shows the statistics and characteristics of the original dataset and the Hemoglobin concentration level (g/dL) used for the study. Figures 5 and 6 show the marked ROI and the extracted ROI of the images respectively.

3.2 | Image augmentation

For higher accuracy to be derived, machine learning models need to be trained on a large dataset. The small size of the dataset is capable of resulting in overfitting.[37] This is due to the reason that during the training and testing stage, data

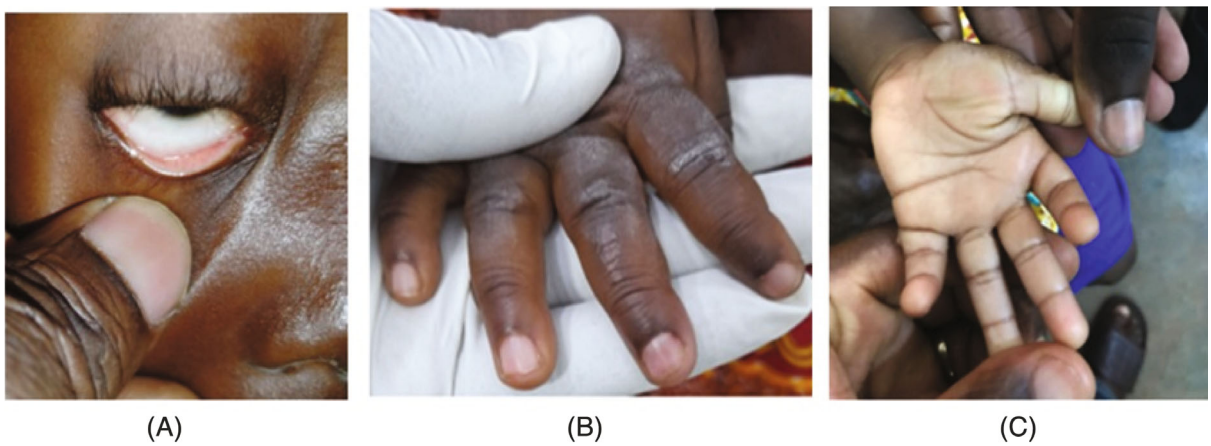

FIGURE 3 Image description of how the dataset photographs were taken.

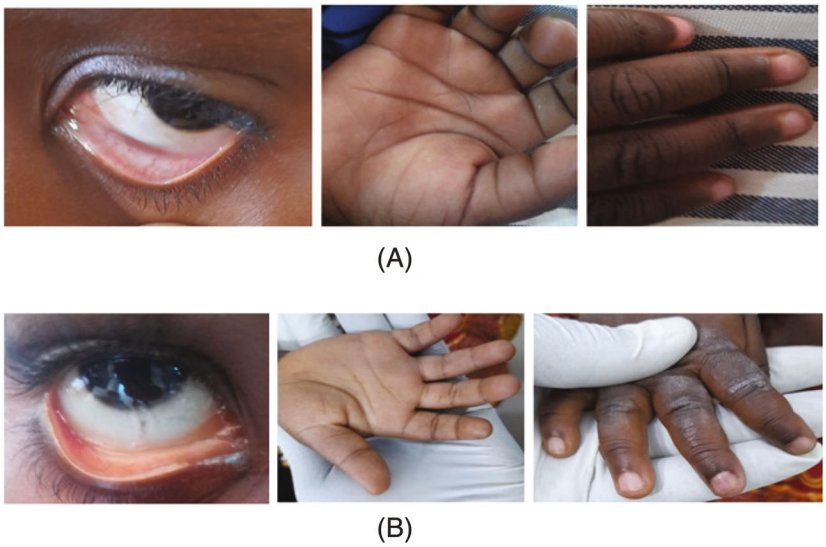

FIGURE 4 Raw images of the conjunctiva of the eyes, palpable palm, and color of the fingernails, where (A) is for non-anemic images and (B) is for anemic images.

TABLE 2 Samples of biodata (dataset) collected from selected participants for the study.

Image ID	Hb Level	Age	Gender	Remarks
Image 001	8.9	2	Male	Anemic
Image 002	12	5	Male	Non-anemic
Image 003	12	4	Female	Non-anemic
Image 004	12	4	Male	Non-anemic
Image 005	9.9	5	Male	Anemic
Image 006	12	1	Female	Non-anemic
Image 007	12	1	Male	Non-anemic
Image 008	12.5	3	Female	Non-anemic
Image 009	9.9	4	Male	Anemic
Image 010	12	2	Female	Non-anemic
Image 011	8.9	4	Male	Anemic
Image 012	9.9	3	Female	Anemic
Image 013	8.9	2	Female	Anemic
Image 014	8.95	2	Male	Anemic
Image 015	12	2	Female	Non-anemic
Image 016	12.5	5	Male	Non-anemic

samples that are small in number are not able to be generalized and used for hyperparameter models. Table 4 gives details of the original dataset while Table 5 gives details of the dataset size after the application of the image augmentation technique.

Image augmentation techniques are used to execute procedurals on images that are artificially generated such as rotation, shift, flip, translation and so forth. Anemia dataset is hard to come by, as a result, this study uses image argumentation to expand the dataset sample for training, testing and validation of the model.

TABLE 3 Statistics and characteristics on the original dataset and the hemoglobin concentration level (g/dL).

	Patient class and characteristics on dataset		
	Anemic	**Non-anemic**	**Total**
Patients	424 (60%)	286 (40%)	710 (100%)
Female	174 (57%)	132 (43%)	306 (43%)
Male	250 (62%)	154 (38%)	404 (57%)
Age (months)	6–59 months		
Anemia classification	Anemic	Non-anemic	
Hemoglobin levels	<11 g/dL	>=11 g/dL	

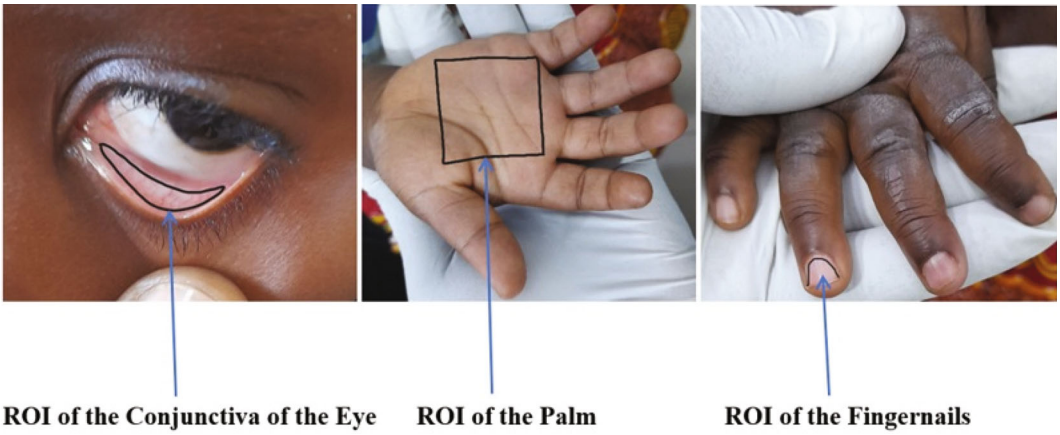

FIGURE 5 Region of interest (ROI) of image.

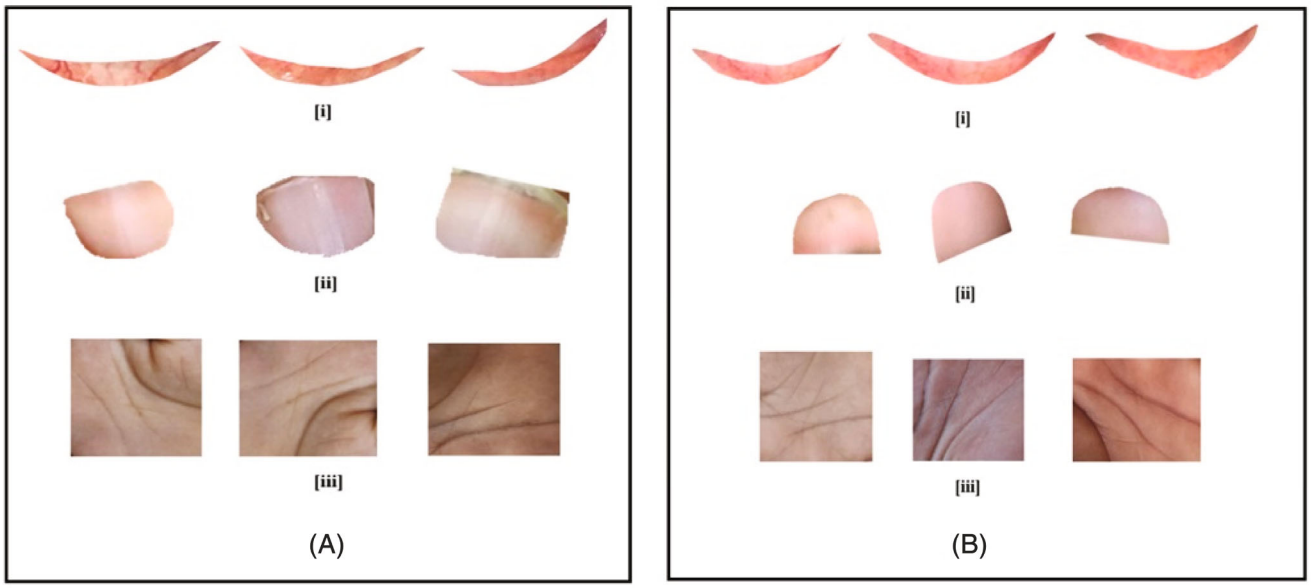

FIGURE 6 Sample of extracted images where (A) are anemic images and (B) are non-anemic images. (i)–(iii) are conjunctiva of the eyes, the color of the fingernails, and the palpable palm respectively, for both (A) and (B) (anemic and non-anemic) images.

TABLE 4 Original image dataset for the detection of anemia.

Original image dataset	Anemic	Non-anemic	Total dataset
Conjunctiva of the eyes	424	286	710
Palpable palms	424	286	710
Color of the fingernails	424	286	710

TABLE 5 Dataset after image augmentation for the detection of anemia.

Dataset after image augmentation	Anemic	Non-anemic	Total dataset
Conjunctiva of the eyes	1520	1115	2635
Palpable palms	1520	1115	2635
Color of the fingernails	1520	1115	2635
Total	4560	3345	7905

- **Rotation**: in the rotation of the image augmentation, the actual image is rotated 90°, and 270° to acquire the artificial image with the values of the mean intensity of the image remaining the same as the positioning of the images varies. The mathematical model for rotation image augmentation is indicated in Equations (1)–(5).

The rotation angle θ for the equations for the new coordinates of a pixel is defined as:

$$x' = x\cos\theta - y\sin\theta \tag{1}$$

$$y' = x\sin\theta + y\cos\theta \tag{2}$$

in an anti-clockwise rotation. In an analogous formulation, the position of every pixel (x', y') in the new image can be written as a vector and the rotation matrix:

$$\begin{matrix} x' \\ y' \end{matrix}\begin{bmatrix} x' \\ y' \end{bmatrix} = \begin{bmatrix} \cos\theta & -\sin\theta \\ \sin\theta & \cos\theta \end{bmatrix}\begin{bmatrix} x \\ y \end{bmatrix} \tag{3}$$

The rotation (x_0, y_0) is the coordinates $(0, 0)$ point of derivation which rotates at the mid-point of the image or around a certain point. For an image or a pixel to rotate around a point (x_0, y_0) subjectively the equation is expressed as;

$$x' = x_0 + (x - x_0)\cos\theta + (y - y_0)\sin\theta. \tag{4}$$

$$y' = y_0 + (x - x_0)\,Sin\theta + (y - y_0)\cos\theta. \tag{5}$$

The pixel at the position (x_0, y_0) is the only pixel that does not move from its position. If an additional image is intended from the original image one, x and y then describe the equation which needs to be solved.

- **Flipping:** For the enhancement of different forms of artificial images, the original images can be vertically or horizontally flipped as the positioning of this operation is altered, while the features and components of the values of the mean intensity remain unchanged.

The inverse of the coordinates places the new image outside the old image, and where there is the ought for the image to be flipped or mirrored along the y-axis, the new image presented requires to be translated also by the image height. The mathematical models for the flipping technique are stated in Equations (6)–(7).

$$x' = x, \tag{6}$$

$$y' = y_{\max} - y. \tag{7}$$

The operations only operate integers of the coordinates and the margins of the image which are new to be ordinarily equal to the old image margins without any interruption.

- **Translation:** the ROI of the actual images are marginally shifted to either the X and Y directions or mutually. The translation operation does not change the values of the image component of the mean intensity.

The mathematical models for translation in image augmentation are enlisted in Equations (8) and (9).

$$x' = x + xT, \tag{8}$$

$$y' = y + yT, \tag{9}$$

where the original coordinates of x and y are the coordinates of $x'$and y' in the new image denoted by the coordinates of a pixel $\boldsymbol{P}$, as $\boldsymbol{P}$ is translated by a distance in every direction expressed as $\boldsymbol{xT}$ and $\boldsymbol{yT}$ correspondingly.

In the process of augmenting the images, the original datasets for each image, (the conjunctiva of the eyes, palpable palm and the fingernails) were rotated 90°, and 270°, flipped (mirrored/mirroring) which was done using the vertical and horizontal method and utilized a translation to the X and Y axis.

Some operations in image augmentation such as Gaussian and cropping are not suitable since they significantly adjust the value of the mean intensity of the image components.[37] After the augmentation of the images was completed, the final datasets in Table 5 were used.

Afterwards, a random selection technique was used to divide the dataset for training which consists of 70% of the total dataset used for training, 10% for validation and 20% for testing as detailed in Table 5. The size of the dataset for the conjunctiva of the eye, palm and fingernails were of the same data size. All three images were from the same patient/person, and when one of the images (either the conjunctiva, palm, or fingernails) was rejected, all the remaining images from the patient/person were also rejected.

3.3 | Machine learning models utilized for the study

3.3.1 | Decision trees

The decision tree algorithm is effective for the analysis of several variables even though they are simple. Splitting data into branch-like segments is identified by various mechanisms depending on the algorithm used to operate.[38] Every branch of the tree represents the value of each attribute, whereas the attribute represents each node of the tree. The minimum number of instances in the leaf was set to 10 and a minimum of 100 trees, while smaller subsets of less than 5 were not divided and were used as the limit in the binary tree.

3.3.2 | Naïve Bayes

With the use of probability based on a given set of features, the Naïve Bayes classifier allows one to predict a class or category and is termed a probabilistic classifier because it incorporates strong independence assumptions based on models of probability.[22] Because there are no hyperparameters to adjust, the Nave Bayes typically generalizes effectively.[7]

3.3.3 | k-nearest neighbor (k-NN) algorithm

The K-NN algorithm is a supervised ML algorithm which is simple and capable of being used to handle both problems of regression and classification. Even though it has a major drawback of significantly as the data size to be used grows it slows down, and it is easy to be implemented and to be understood.[38,40]

The k-NN used 100 neighbors and the metric was set to Euclidean with uniform weight while the optimal instance is $k = 2$ which was assigned to the nearest neighbor in the class. This method computes the distance between the feature vectors and their nearest neighbors and does not produce duplicates, instead providing synthetic data points that differ slightly from the actual data points.[6,41]

3.3.4 | Support vector machine (SVM)

SVMs are a relatively new and widely used family of classification tools that combine several elements of previously used methods. SVMs, like discriminant analysis, start with the assumption that the data are "separable," that is, that they can be split into groups by a functional separator.[42] The Sigmoid was used for the operation with 100 iterations as the limit, cost (c) = 100 and epsilon of regression (ε) was assigned to 1.10 while the numerical tolerance was set to 0.1000.

3.3.5 | Convolutional neural network

In CNN, the features of images are identified by filters more than once to permit the categorization of objects. There is a kernel edge in the CNN that uses differential values of large pixels to highlight pixels, as these features are extracted with the CNN scheme responsible for the kernel.[43] The CNN was trained using the AlexNet and the stochastic gradient descent (SGD) optimization and ReLu. The activation function has a regularization of a = 0.0001 and a maximum iteration of 10. The activation function's major function is to turn the nodes' signal inputs into signal outputs. The CNN would devolve into a linear regression in the absence of the activation function, rendering it incapable of training complicated models.[7]

3.4 | Anemia detection condition

After pre-processing of images to generate the dataset, the extracted ROI were transformed in the CIELAB (also known as CIE L*a*b*) color space model for each image. The L*a*b color space is envisioned to mimic human vision or perception. It is expressed by the standard deviation value of the ROI a* elements, which is the mean value. The red components (a* > 0) and green components (a* 0) are instances of a* components.

Preceding work in this field illustrates that there exists a resilient affiliation between a* components and Hb levels when calculated using Pearson correlation index, and various experiments done in this area show that patients with higher values of Hb verge to have an average value of a* greater than 160 and patients with lower Hb values tend to have an average value of a* less than 142.[44] As a result, the average values of a* components seem to be more discerning (i.e., the mean intensity of red and green components better differentiates anemic and non-anemic individuals).

To activate the color characterization, the images were operated using the CIE L*a*b* color space. This color space maps all visible to the human eye hues into a three-dimensional integer space enabling device-independent digital representation. The goal of these characterizations is to accurately measure human vision, that is, the images' non-linear approach: standardized changes with time because the aforementioned components correspond to systematic changes in the purported color.

The relative perceptual differences between two colors in L*, a*, b* may be calculated and approximated by treating each color as a point in a three-dimensional space (with three components: L* a*b*) and taking the Euclidean distance between them. The three coordinates L*, a*, and b* are prevalently constant to a predetermined distance. L* (lightness) represents the darkest black at 0 and the brightest white at 100, whereas a* and b* are color channels.

The actuality in the Cartesian coordinate system (a*, b*) characterizes nonalignment as gray. The colors of the foe are displayed on the a* axis, with red at a* > 0 and green at a* 0, while the colors of the opponent are depicted on the b* axis, with yellow at b* > 0 and blue at b* 0. To determine the confidence redness of the images, the positive a* values are good indications.[45]

Every RGB triplet is translated to a discrete numerical value that reflects the red intensity of the color as viewed using the perception of human vision to examine the link between the acquired image and the Hb readings of a patient. The initial image is converted to RGB → CIE L*a*b* color scale (RGB color component mapped to CIE L*a*b* color space).

After several experiments, the best detection result was obtained by combining three component features in total, namely a*, b*, and the G value retrieved from the RGB component pictures. The L and the values of the RGB components were utilized to filter the input data. The mean values of the attributes a*, b*, and G were determined precisely by taking into account just the picture pixels with minL<L < maxL and min < R = G = B < max.

This filtering ensures that picture pixels that are excessively dark or bright are removed, and so the approach given here considers only pixels that allow an accurate pallor assessment of the images. The Equations (10)–(13) are the mathematical models for the CIE L*a*b* color space demonstration.

$$L^* = 116f\left(\frac{Y}{Yn}\right) - 16, \tag{10}$$

$$a^* = 500\left\{f\left(\frac{X}{Xn}\right) - f\left(\frac{Y}{Yn}\right)\right\}, \tag{11}$$

$$b^* = 200\left\{f\left(\frac{X}{Xn}\right) - f\left(\frac{Z}{Zn}\right)\right\}, \tag{12}$$

where $f(s) = s^{\frac{1}{3}}$, for $s > 0.008856$
And $f(s) = 7.787s + \frac{16}{116}$, for $s \leq 0.008856$
The color difference ΔE between two colors in the CIE L*a*b* (CIELAB) color space is;

$$\Delta E = \sqrt{\left(L_2^* - L_1^*\right)^2 + \left(a_2^* - a_1^*\right)^2 + \left(b_2^* - b_1^*\right)^2}, \tag{13}$$

where the ΔE unity value denotes a just noticeable difference.

3.5 | Experimental setup

In this study, five machine learning algorithms (Naïve Bayes, k-NN, SVM, CNN, and decision tree) were used to detect anemia using images of the conjunctiva of the eye, palpable palm and color of the fingernails. The datasets used were obtained from 710 participants. The images were augmented to 2635 for each (conjunctiva of the eye, palpable palm and color of the fingernails).

The dataset was randomly divided into 70%, 10% and 20%, and was utilized to train, validated, and tested the models respectively. We employed a 10-fold cross-validation for validating the models. Cross-validation is a modest and effective approach used for classification/detection techniques to evaluate performance. The CNN was trained with the SGD optimization and ReLu as the activation function with a regularization of $a = 0.0001$, with an iteration maximal of 10. The prime function of the activation function is for converting the signal input of the nodes into a signal output. The CNN would become a linear regression with the absence of the activation function, which would not be proficient in learning models which are complex.

For SVM, Sigmoid was used for the operation with 100 iterations as the limit, cost (c) = 100 and epsilon of regression (ε) was assigned to 1.10 while the numerical tolerance was set to 0.1000. The k-NN had 100 number of neighbors as the metric was set to Euclidean with uniform weight. For the decision tree, we induced the binary tree minimal number of instances in the leave to 10, while smaller subsets less than 5 were not split and 100 minimal of the trees as the limit.

The experiment was carried out using the Orange Data Mining tool (Version 3.32) on Windows 11 (Enterprise Version) Microsoft Cooperation computer system, 64-bit OS, Intel Core i3 2.4 and 2.5 GHz processor (8th Generation), 128 solid-state drive (SSD) and a 4GB RAM. Orange is a robust data mining and machine learning toolkit through the use of visual and python programming devised in the late 1990s by the University of Ljubljana at the Bioinformatics Laboratory, Department of Computer and Information Science.

Naik and Samant,[46] used machine learning algorithms such as Naïve Bayes, k-NN and decision tree to detect liver disorder of which the orange data mining software gave a significant result. Similarly, Verma and Arjun,[23] used orange data mining software to diagnose and detect diabetes with the use of random forest, ANN, k-NN, SVM, and decision tree algorithms. The ANN achieved the highest accuracy of 90.27%, whereas the least accuracy among the other algorithms was SVM with 64.66% accuracy. This justifies that orange data mining software is efficient and effective for the detection of diseases such as anemia, diabetes and liver disorder.

3.6 | Performance measures

For the performance of the models to be evaluated, AUC, F1—score, precision, and recall were used with a 10-fold validation in the anemia detection models with their mathematical formulas stated in Equations (14)–(19).

$$\text{Accuracy} = \frac{\text{TP} + \text{TN}}{\text{TP} + \text{TN} + \text{FP} + \text{FN}}, \tag{14}$$

$$\text{Recall} = \frac{\text{TP}}{\text{TP} + \text{FN}}, \tag{15}$$

$$\text{Specificity} = \frac{\text{TN}}{\text{TN} + \text{FP}}, \tag{16}$$

$$\text{Precision} = \frac{\text{TP}}{\text{TP} + \text{FP}}, \tag{17}$$

$$\text{AUC}\ (TPR) = \frac{\text{TP}}{\text{TP} + \text{FN}}, \tag{18}$$

$$\text{F1} - \text{score} = \frac{2(P.R)}{P + R}, \tag{19}$$

where; TP is the true positive number of samples when predicted and the real values are positive.
TN is the true negative, FN is the false negative, P is the precision, R is the recall and TNR is the true negative rate.

4 | RESULTS

After the models were trained, validated, and tested on the datasets, the proposed models obtained a significant result. The CNN obtained an accuracy of 98.45% on the conjunctiva of the eyes, 98.33% on the color of the fingernails, and 99.12% on the palpable palm. The SVM had the lowest accuracy of 89.45% for the conjunctiva of the eyes, 92.96% for the color of the fingernails and 95.34% for the palpable palm. Tables 6–8 gives details of the results obtained when the models were tested with their corresponding evaluation metrics, while Figures 7–9 give a graphical representation of the models' performance.

4.1 | Discussion

For the performance of machine learning models to be evaluated, accuracy, F1-score, AUC, precision, and recall were well-thought-out procedures for evaluating the models. To avoid overfitting of performance for the detection by the models, we utilized a 10-fold cross-validation and validated the models.

TABLE 6 Performance of the proposed models in detecting anemia using conjunctiva of the eyes.

		Conjunctiva of the eyes (%)				
S/N	**Algorithm**	**Accuracy**	**F1-score**	**AUC**	**Precision**	**Recall**
1	CNN	98.45	97.63	99.93	97.64	97.63
2	Naïve Bayes	94.94	92.24	97.74	92.64	91.84
3	Decision tree	97.32	96.02	97.70	93.67	98.49
4	k-NN	97.96	96.86	99.86	97.60	96.13
5	SVM	89.45	84.53	92.16	81.34	87.98

TABLE 7 Performance of the proposed models in detecting anemia using fingernails.

		Color of the fingernails (%)				
S/N	**Algorithm**	**Accuracy**	**F1-score**	**AUC**	**Precision**	**Recall**
1	CNN	98.33	97.54	99.93	97.64	97.44
2	Naïve Bayes	94.94	92.35	98.01	91.96	92.75
3	Decision tree	97.18	95.61	97.59	98.41	92.96
4	k-NN	97.89	96.82	99.83	96.21	97.44
5	SVM	92.69	88.62	97.08	91.01	86.35

TABLE 8 Performance of the proposed models in the detection of anemia using a palpable palm.

		Palpable palm (%)				
S/N	**Algorithm**	**Accuracy**	**F1-score**	**AUC**	**Precision**	**Recall**
1	CNN	99.12	99.89	99.95	99.79	99.98
2	Naïve Bayes	98.96	99.97	99.98	99.97	99.93
3	Decision tree	98.29	98.97	99.38	98.77	99.18
4	k-NN	98.92	99.89	99.98	99.79	99.92
5	SVM	95.34	94.59	98.97	95.99	93.23

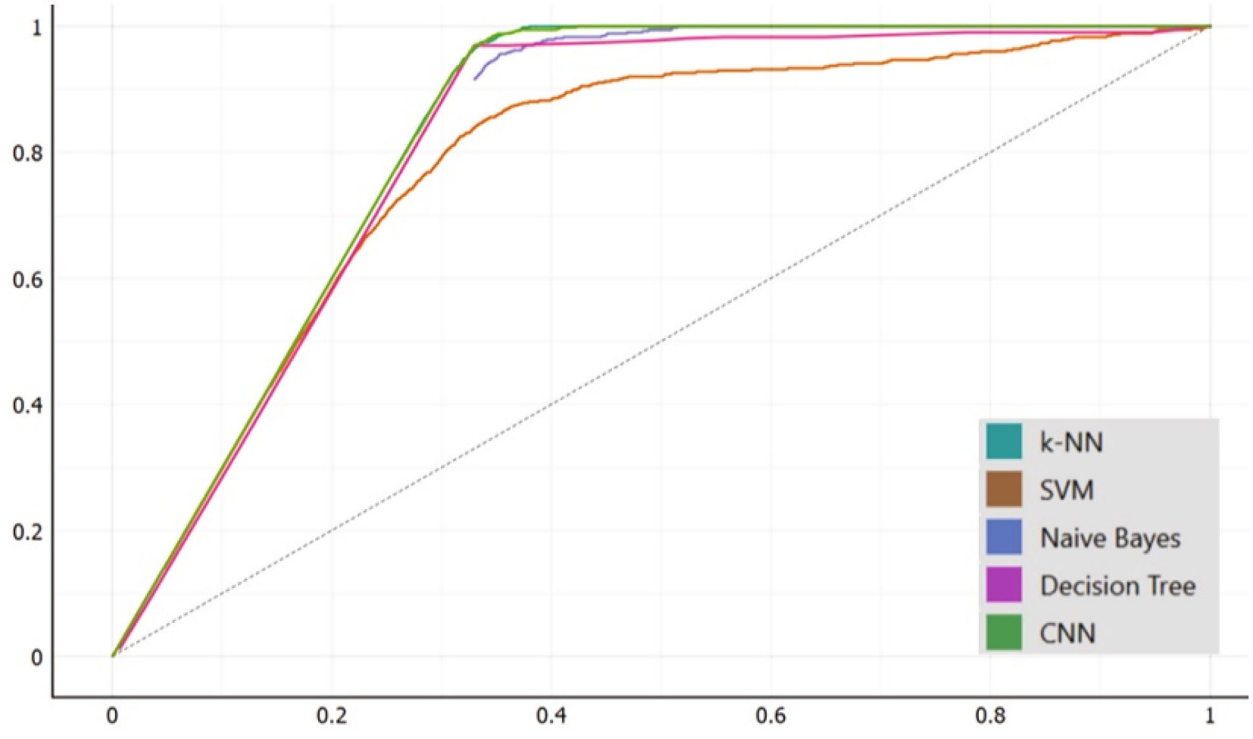

FIGURE 7 AUC curve of the conjunctiva of the eyes for anemia detection.

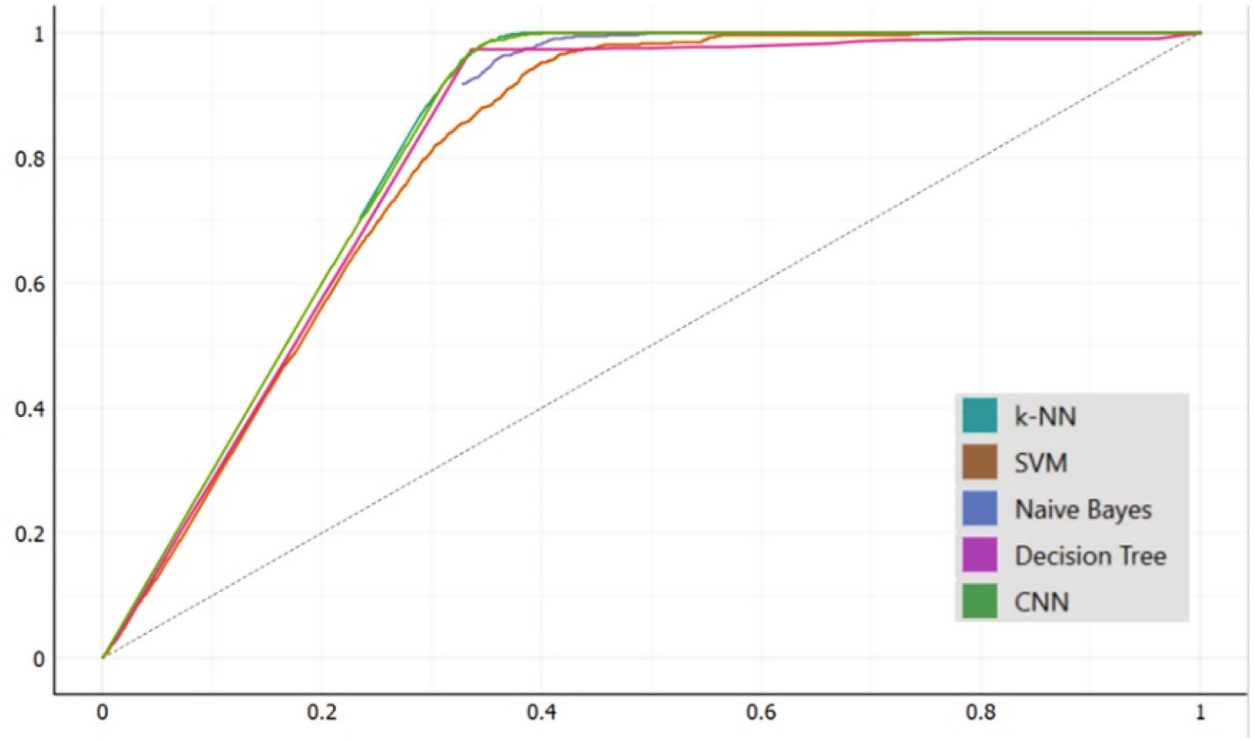

FIGURE 8 AUC curve of the fingernails in anemia detection.

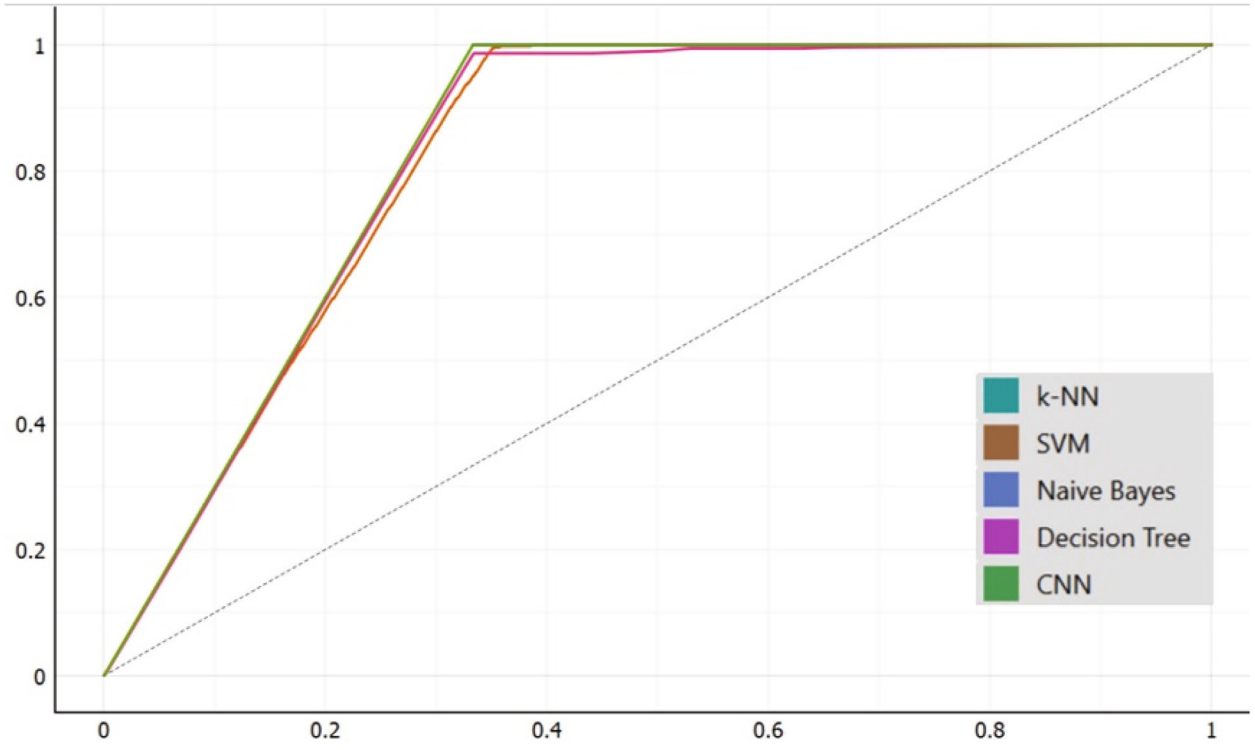

FIGURE 9 AUC curve of the palm in anemia detection.

The results of the various algorithms for the detection of anemia were considered. The Naïve Bayes achieved the highest accuracy of 98.96% when tested on the palpable palm, although the CNN had an accuracy of 99.12%. The SVM attained the lowest accuracy of 95.34%. The Naïve Bayes, decision tree and k-NN obtained an accuracy of 98.96%, 98.29%, and 98.92% respectively when tested on the palpable palm dataset.

However, a CNN approach was utilized by Emmanuel et al.[30] to detect anemia which had an accuracy of 89.33%, while Reference 37 applied ANN technique and achieved an accuracy of 97.00%, and 90.00% accuracy was achieved by Peksi et al.[22] when a Naïve Bayes algorithm was used to detect anemia as indicated in Table 9. Tables 6–8 give details of the models' performance on the various medical images used for the study with their corresponding evaluation metrics achieved.

There were no significant variations in the performance of the models between the color of the fingernails and the conjunctiva of the eyes when tested by the models. The CNN achieved an accuracy of 98.45% in the conjunctiva and 98.33% in the fingernails. The Decision Tree obtained an accuracy of 97.32%, 97.96%, and 89.45% obtained by the k-NN and the SVM respectively when tested on the conjunctiva of the eye images. On the other hand, the SVM achieved an accuracy of 92.69%, while the k-NN, decision tree, and Naïve Bayes achieved an accuracy of 97.89%, 97.18 and 94.94, respectively, when tested on the color of the fingernails dataset. Figures 7–9 give a graphical representation of the various performance achieved by the models when trained, validated and tested on the models.

Divya et al.[39] indicated that pallor (palpable) palmer is the best detector of anemia among the conjunctiva, fingernails, and tongue. Appiahene et al.[7] also stated that the palpable palm gives a significant accuracy in the detection of anemia than the conjunctiva of the eyes, mostly for children under the age of 5–59 months, even though the conjunctiva of the eyes is mostly used for the detection of anemia, especially with the use of the non-invasive method.

Divya et al.[39] detected anemia by evaluating the effectiveness of the conjunctiva, tongue, nailbed (fingernails), and the palm[48] on their etiology relationship. The study showed that the palm had higher accuracy to detect anemia, followed by the conjunctiva and then the fingernails, while the tongue gave the least accuracy. Getaneh et al.[49] conducted a study on anemia detection using the pallor of the conjunctiva, tongue, nailbed, and palm. The datasets were derived from children (participants) of 6–59 months. The results obtained by Getaneh et al.[49] concluded that the palm achieved the highest sensitivity of 58% to detect anemia which was moderated and when combined with the conjunctiva and palm sensitivity was increased to 73%.

This study has contributed to knowledge through the use of multiple medical images of the conjunctiva of the eyes, palpable palm and color of the fingernails in the detection of anemia. In addition, there has been a comparative study based on the models' performance which has been concluded and supported by other studies such as References 7,39,49,50 that the palpable palm is an ideal feature to detect anemia in children since it is easy to be accessed as compared to the conjunctiva of the eye which might expose a child's eye to a falling object or particle.

This can also cause a risk of infection in children when using the conjunctiva of the eye to detect anemia since the finger can enter the eye when they access the conjunctiva of the eye. Moreover, this study has used an extensive and diverse dataset higher than the dataset used by the studies reviewed in the literature and Table 1, and our dataset has also been publicly available for future use by other researchers.

The results obtained from the proposed models used in this study are a clear indication that the palm is an accurate part of the human body to be used to detect iron-deficiency anemia mostly in children below the age of 6. Moreso, the CNN performed better than the Naïve Bayes when the conjunctiva and the color of the fingernails were trained, validated and tested. However, the Naïve Bayes performance on the palpable palm was higher than the other models.

TABLE 9 Comparison of other related works results.

Reference	Proposed technique	Algorithm used	Accuracy achieved
Tamir et al.[8]	Clustering (unsupervised learning)	RGB thresholding algorithm	78.90%
Dimauro et al.[10]	Classification (supervised learning)	k-NN	90.26%
Peksi et al.[22]	Classification (supervised learning)	Naïve Bayes	90%
Dada et al.[30]	Classification (supervised learning)	CNN	89.33%.
Jain et al.[37]	Classification (supervised learning)	ANN	97.00%
Sevani et al.[47]	Clustering (unsupervised learning)	k-means	90%

4.2 | Conclusion

This article aimed to detect iron deficiency anemia, comparing machine learning models (CNN, Naïve Bayes, decision tree, k-NN and SVM) performance with the use of medical images. The models were trained, validated, and tested on images of the conjunctiva of the eyes, palpable palm and color of the fingernails.

The CNN had a higher accuracy than all the models when tested on the fingernails, palpable palm, and conjunctiva images. The results obtained by the models show that the CNN is robust and performs better than Naïve Bayes, decision tree, k-NN and SVM in anemia detection and the palpable palm is one of the reliable human features for anemia detection in children due to its higher detection accuracy.

Furthermore, the performance of the models on the palm had a higher accuracy than that of the fingernails and conjunctiva when tested with the data set. The palm is simple to examine compared to the eyes, which is challenging to access the conjunctiva and the ROI, particularly for children below 6 years whose eyes may often be exposed to falling. Additionally, minors' eyes would be opened to take pictures or examine the conjunctiva of the eyes directly. There is a chance that someone's finger could get in their eyes.[7] This can be a potential infection source.

The performance of the models would have a great impact on the health facilities concerning the detection of iron-deficiency anemia due to the effectiveness and efficient performance of the proposed models. The massive performance of the models obtained by this study would have a great impact on health facilities worldwide, especially in health facilities in rural Ghana where access to health facilities, equipment or resources and health professionals is scarce.

However, this study is limited to the development and deployment of a mobile application to enhance its usage, this would be considered a future work. Future works would consider the development of a mobile application in which the proposed models developed would be integrated to enhance easy access and use.

AUTHOR CONTRIBUTIONS

Peter Appiahene analyzed the data, conception, or design of the work. Justice Williams Asare collected the data and analyzed the algorithms. Emmanuel Timmy Donkoh and Giovanni Dimauro analyzed the data for interpretation and critically analyzed the article. All authors read and approved the article.

CONFLICT OF INTEREST STATEMENT

The authors assert that they do not have a conflict of interest in any form in this study.

PEER REVIEW

The peer review history for this article is available at https://www.webofscience.com/api/gateway/wos/peer-review/10.1002/eng2.12667.

DATA AVAILABILITY STATEMENT

The datasets used for this study have been published in a repository as listed below:

1. Asare JW, Appiahene P, Donkoh E. Detection of anemia using colour of the fingernails image datasets from Ghana. *Mendeley Data*. 2022;V1. doi:10.17632/2xx4j3kjg2.1
2. Asare JW, Appiahene P, Donkoh E. Anemia detection using palpable palm image datasets from Ghana. *Mendeley Data*. 2022;V1. doi:10.17632/ccr8cm22vz.1
3. Appiahene P, Asare JW, Donkoh E. Application of machine learning in detecting iron deficiency anemia using conjunctiva image dataset from Ghana. *Mendeley Data*. 2022;V1. doi:10.17632/nt7r8hv2pz.1

ETHICS STATEMENT

The ethics committee of the hospitals enlisted in this study approved the collection of the dataset before the study started. Moreover, since the participants (patients) used for the study were minors, ethical consent was requested from their parent(s) or guardian(s) and the aim and objectives of the study were discussed with them with the benefits it would be the health services. Consent was approved by their parents (parents) or guardians (children) before the participants were enrolled in data collection. In addition, the Committee for Human Research and Ethics (CHRE) at the University of Energy and Natural Resources, Sunyani approved (Reference number: CHRE/CA/042/22) the commencement of this

work. Furthermore, the names and faces of the patients or participants were not shown or exposed during the capture of the images, which makes their identities unknown.

ORCID

Justice Williams Asare https://orcid.org/0000-0002-5781-1213
Peter Appiahene https://orcid.org/0000-0002-6098-4537

REFERENCE

1. WHO. Anemia Treatment, prevalence and data status. October 12, 2019. Accessed July 16, 2022. https://www.who.int/health-topics/anaemia#tab=tab_3
2. Al-Alimi AA, Bashanfer S, Morish MA. Prevalence of iron deficiency anemia among university students in Hodeida Province, Yemen. *Anemia*. 2018;2018:1-7. doi:10.1155/2018/4157876
3. Pasricha S-R, Tye-Din J, Muckenthaler MU, Swinkels DW. Iron deficiency. *Lancet*. 2021;397(10270):233-248. doi:10.1016/s0140-6736(20)32594-0
4. Tartan EO, Berkol A, Ekici Y. Anemia diagnosis by using artificial neural networks. *Int J Multidiscip Stud Innov Technol*. 2020;4(1):14-17.
5. Saputra DCE, Sunat K, Ratnaningsih T. A new artificial intelligence approach using extreme learning machine as the potentially effective model to predict and analyze the diagnosis of anemia. *Healthcare*. 2023;11(5):697. doi:10.3390/healthcare11050697
6. Dithy MD, Krishnapriya V. Anemia selection in pregnant women by using random prediction (Rp) classification algorithm. *Int J Recent Technol Eng*. 2019;8(2):2623-2630. doi:10.35940/ijrte.B3016.078219
7. Appiahene P, Asare JW, Donkoh ET, Dimauro G, Maglietta R. Detection of iron deficiency anemia by medical images: a comparative study of machine learning algorithms. *BioData Min*. 2023;16(1):2. doi:10.1186/s13040-023-00319-z
8. Tamir A, Jahan CS, Saif MS, et al. Detection of anemia from image of the anterior conjunctiva of the eye by image processing and thresholding. Proceedings of the 2017 IEEE Region 10 Humanitarian Technology Conference (R10-HTC); December 2017: 697–701. doi:10.1109/R10-HTC.2017.8289053
9. Tetschke M, Lilienthal P, Pottgiesser T, Fischer T, Schalk E, Sager S. Mathematical modeling of RBC count dynamics after blood loss. *Processes*. 2018;6(9):157. doi:10.3390/pr6090157
10. Dimauro G, Caivano D, Girardi F. A new method and a non-invasive device to estimate anemia based on digital images of the conjunctiva. *IEEE Access*. 2018;6:46968-46975. doi:10.1109/ACCESS.2018.2867110
11. Wiafe MA, Ayenu J, Eli-Cophie D. A review of the risk factors for iron deficiency Anaemia among adolescents in developing countries. *Anemia*. 2023;2023:1-11. doi:10.1155/2023/6406286
12. Who has the highest risk of developing anemia? 2019. https://www.ekfdiagnostics.com/who-has-the-highest-risk-of-developing-anemia.html
13. World Health Organization. Anemia treatment, prevalence and data status. April 2019. Accessed July 16, 2022. https://www.who.int/health-topics/anaemia#tab=tab_3
14. Dimauro G, Guarini A, Caivano D, Girardi F, Pasciolla C, Iacobazzi A. Detecting clinical signs of anaemia from digital images of the palpebral conjunctiva. *IEEE Access*. 2019;7:113488-113498. doi:10.1109/access.2019.2932274
15. Mitani A, Huang A, Venugopalan S, et al. Detection of anaemia from retinal fundus images via deep learning. *Nat Biomed Eng*. 2020;4(1):18-27. doi:10.1038/s41551-019-0487-z
16. Mazzu-Nascimento T, Evangelista DN, Abubakar O, et al. Smartphone-based photo analysis for the evaluation of anemia, jaundice and COVID-19. *Int J Nutrol*. 2021;14(02):e55-e60. doi:10.1055/s-0041-1734014
17. Kasiviswanathan S, Bai Vijayan T, Simone L, Dimauro G. Semantic segmentation of conjunctiva region for non-invasive anemia detection applications. *Electronics*. 2020;9(8):1309. doi:10.3390/electronics9081309
18. Tadesse SE, Zerga AA, Mekonnen TC, et al. Burden and determinants of anemia among under-five children in Africa: systematic review and meta-analysis. *Anemia*. 2022;2022:1-9. doi:10.1155/2022/1382940
19. Mannino RG, Myers DR, Tyburski EA, et al. Smartphone app for non-invasive detection of anemia using only patient-sourced photos. *Nat Commun*. 2018;9(1):4924. doi:10.1038/s41467-018-07262-2
20. Kesavaraj G, Sukumaran S. A study on classification techniques in data mining. Proceedings of the 2013 Fourth International Conference on Computing, Communications and Networking Technologies (ICCCNT); 2013. doi:10.1109/icccnt.2013.6726842
21. Karagül Yıldız T, Yurtay N, Öneç B. Classifying anemia types using artificial learning methods. *Eng Sci Technol Int J*. 2021;24(1):50-70. doi:10.1016/j.jestch.2020.12.003
22. Peksi NJ, Yuwono B, Florestiyanto MY. Classification of anemia with digital images of nails and palms using the naive Bayes method. *Telematika*. 2021;18(1):118. doi:10.31315/telematika.v18i1.4587
23. Dr JV, Arjun P. Diabetes mellitus prediction using ensemble machine learning techniques. *Int J Recent Technol Eng*. 2020;9(2):312-316. doi:10.35940/ijrte.b3480.079220
24. Irum A, Akram M, Ayub SM, Waseem S, Khan MJ. Anemia detection using image processing. Proceedings of the International Conference on Digital Information Processing, Electronics, and Wireless Communications; 2016.
25. Chen Y, Zhong K, Zhu Y, Sun Q. Two-stage hemoglobin prediction based on prior causality. *Front Public Health*. 2022;10:1079389. doi:10.3389/fpubh.2022.1079389

26. Sarsam SM, Al-Samarraie H, Alzahrani AI, Shibghatullah AS. A non-invasive machine learning mechanism for early disease recognition on twitter: the case of anemia. *Artif Intell Med*. 2022;134:102428. doi:10.1016/j.artmed.2022.102428
27. Shahzad M, Umar AI, Shirazi SH, et al. Identification of anemia and its severity level in a peripheral blood smear using 3-tier deep neural network. *Appl Sci*. 2022;12(10):5030. doi:10.3390/app12105030
28. Yeruva S, Varalakshmi MS, Gowtham BP, Chandana YH, Prasad PESNK. Identification of sickle cell anemia using deep neural networks. *Emerg Sci J*. 2021;5(2):200-210. doi:10.28991/esj-2021-01270
29. Dimauro G, Camporeale MG, Dipalma A, Guarini A, Maglietta R. Anaemia detection based on sclera and blood vessel colour estimation. *Biomed Signal Process Control*. 2023;81:104489. doi:10.1016/j.bspc.2022.104489
30. Emmanuel DG, David OO, Stephen JB. Deep convolutional neural network model for detection of sickle cell anemia in peripheral blood images. *Commun Phys Sci*. 2022;8(1):9-22.
31. Magdalena R, Saidah S, Ubaidah IDS, Fuadah YN, Herman N, Ibrahim N. Convolutional neural network for anemia detection based on conjunctiva palpebral images. *J Tek Inform*. 2022;3(2):349-354.
32. Ghosh A, Mukherjee J, Chakravorty N. A low-cost test for anemia using an artificial neural network. *Comput Methods Programs Biomed*. 2023;229:107251. doi:10.1016/j.cmpb.2022.107251
33. Wightman Rojas PM, Mass Noriega LA, Salazar Silva A. Hemoglobin screening using cloud based mobile photography applications. *Ing Univ*. 2019;23(2). doi:10.11144/Javeriana.iyu23-2.hsuc
34. Delgado-Rivera G, Roman-Gonzalez A, Alva-Mantari A, et al. Method for the automatic segmentation of the palpebral conjunctiva using image processing. Proceedings of the 2018 IEEE International Conference on Automation/XXIII Congress of the Chilean Association of Automatic Control (ICA-ACCA); 2018:1-4.
35. Acar E, Türk Ö, Ertuğrul ÖF, Aldemir E. Employing deep learning architectures for image-based automatic cataract diagnosis. *Turk J Electr Eng Comput Sci*. 2021;29(SI-1):2649-2662. doi:10.3906/elk-2103-77
36. Yadav P, Singh NP. Classification of normal and abnormal retinal images by using feature-based machine learning approach. In: Khare A, Tiwary U, Sethi I, Singh N, eds. *Recent Trends in Communication, Computing, and Electronics*. Springer; 2019:387-396. doi:10.1007/978-981-13-2685-1_37
37. Jain P, Bauskar S, Gyanchandani M. Neural network based non-invasive method to detect anemia from images of eye conjunctiva. *Int J Imaging Syst Technol*. 2019;30(1):112-125. doi:10.1002/ima.22359
38. Roychowdhury S, Sun D, Ren J, Bihis M, Hage P, Rahman H. Screening pallor site images for anemia-like pathologies. Proceedings of the IEEE International Conference on Biomedical Health Informatics; 2017:2017.
39. Divya Krishnan K, Avabratha KS, Shenoy KV, Anand KV. Efficacy of site of pallor to detect anemia and its correlation with etiology in under five children. *Int J Contemp Pediatrics*. 2020;8(1):160. doi:10.18203/2349-3291.ijcp20205429
40. Noor NB, Anwar MS, Dey M. Comparative study between decision tree, SVM and KNN to predict anaemic condition. Proceedings of the 2019 IEEE International Conference on Biomedical Engineering, Computer and Information Technology for Health (BECITHCON); November 2019:24-28. doi:10.1109/BECITHCON48839.2019.9063188
41. Dejene BE, Abuhay TM, Bogale DS. Predicting the level of anemia among Ethiopian pregnant women using homogeneous ensemble machine learning algorithm. *BMC Med Inform Decis Mak*. 2022;22(1):247. doi:10.1186/s12911-022-01992-6
42. Djuric N, Grbovic M, Vucetic S. Distributed confidence-weighted classification on big data platforms. In: Govindaraju V, Raghavan VV, Rao CR, eds. *Handbook of Statistics*. Elsevier; 2015:145-168. doi:10.1016/B978-0-444-63492-4.00007-1
43. Aneja S, Shaham U, Kumar RJ, et al. Deep neural network to predict local failure following stereotactic body radiation therapy: integrating imaging and clinical data to predict outcomes. *Int J Radiat Oncol Biol Phys*. 2017;99(2):S47. doi:10.1016/j.ijrobp.2017.06.120
44. Dalvi PT, Vernekar N. Anemia detection using ensemble learning techniques and statistical models. Proceedings of the 2016 IEEE International Conference on Recent Trends in Electronics, Information and Communication Technology (RTEICT 2016); January 2017:1747-1751. doi:10.1109/RTEICT.2016.7808133
45. Bevilacqua V, Dimauro G, Marino F, et al. A novel approach to evaluate blood parameters using computer vision techniques. Proceedings of the 2016 IEEE International Symposium on Medical Measurements and Applications (MeMeA); May 2016:1–6. doi:10.1109/MeMeA.2016.7533760
46. Naik A, Samant L. Correlation review of classification algorithm using data mining tool: WEKA, Rapidminer, Tanagra, Orange and Knime. *Procedia Comput Sci*. 2016;85:662-668.
47. Sevani N, Fredicia F, Persulessy GBV. Detection anemia based on conjunctiva pallor level using *k-means* algorithm. *IOP Conf Ser Mater Sci Eng*. 2018;420:012101. doi:10.1088/1757-899X/420/1/012101
48. Dimauro G, Griseta ME, Camporeale MG, Clemente F, Guarini A, Maglietta R. An intelligent non-invasive system for automated diagnosis of anemia exploiting a novel dataset. *Artif Intell Med*. 2023;136:102477. doi:10.1016/j.artmed.2022.102477
49. Getaneh T, Girma T, Belachew T, Teklemariam S. The utility of pallor detecting anemia in under five years old children. *Ethiop Med J*. 2000;38(2):77-84.
50. Chand S, Shaikh F, Das C, Memon Y, Nizamani MA, Baloch ZAQ. Anemia in children with palmar pallor aged 02 months to 05 years. *Indo Am J Pharm Sci*. 2017;4(2):290-295.

How to cite this article: Asare JW, Appiahene P, Donkoh ET, Dimauro G. Iron deficiency anemia detection using machine learning models: A comparative study of fingernails, palm and conjunctiva of the eye images. *Engineering Reports*. 2023;5(11):e12667. doi: 10.1002/eng2.12667

APPENDIX A

TABLE A1 List of hospitals where datasets were collected.

Hospital	City/town	Total dataset
Ahmadiyya Muslim Hospital	Tachiman	128
Bolgatanga Regional Hospital	Bolgatanga	95
Ejusu Government Hospital	Ejusu	41
Holy Family Hospital	Berekum	8
Kintampo Municipal Hospital	Kintampo	60
Komfo Anokye Teaching Hospital	Kumasi	134
Manhyia District Hospital	Kumasi	43
Nkawie-Toase Government Hospital	Nkawie-Toase	86
SDA Hospital	Sunyani	15
Sunyani Municipal Hospital	Sunyani	100
Total		710